frontiers | Frontiers in Mechanical Engineering

TYPE Original Research
PUBLISHED 08 January 2026
DOI 10.3389/fmech.2025.1687802

OPEN ACCESS

EDITED BY
Lei Zhang,
Beijing Institute of Technology, China

REVIEWED BY
Jiageng Ruan,
Beijing University of Technology, China
Luttfi A. Al-Haddad,
University of Technology, Iraq
Guohai Liu,
Jiangsu University, China

*CORRESPONDENCE
Zhidong Guo,
gzd_guo@outlook.com

RECEIVED 18 August 2025
REVISED 03 December 2025
ACCEPTED 09 December 2025
PUBLISHED 08 January 2026

CITATION
Guo Z and Pan X (2026) Research on fault diagnosis in the operation monitoring of permanent magnet synchronous motors through deep learning.
Front. Mech. Eng. 11:1687802.
doi: 10.3389/fmech.2025.1687802

Research on fault diagnosis in the operation monitoring of permanent magnet synchronous motors through deep learning

Zhidong Guo* and Xiaobei Pan

Institute of Intelligent Manufacturing, Sanmenxia Polytechnic, Sanmenxia, Henan, China

Background: Permanent magnet synchronous motor (PMSM) may develop faults during long-term operation, affecting the stability and safety of the drive system.
Objective: This paper aims to identify the types of PMSM operation faults using a deep learning algorithm.
Methods: The convolutional neural network (CNN)-gated recurrent unit (GRU) algorithm was compared with the support vector machine (SVM), random forest (RF), and back-propagation neural network (BPNN) algorithms. Ablation experiments were conducted. Finally, the Shapley additive explanations algorithm was used to calculate the importance of feature indicators.
Results: The CNN-GRU algorithm had better fault-diagnosis performance compared with the other three algorithms and was easier to make an accurate diagnosis of inter-turn short-circuit faults in stator windings. The precision, recall rate, and F-score of the CNN-GRU algorithm were 0.950, 0.948, and 0.949, respectively; the corresponding values of the BPNN algorithm were 0.823, 0.819, and 0.821, respectively; the corresponding values of the RF algorithm were 0.719, 0.713, and 0.716, respectively; the corresponding values of the SVM algorithm were 0.707, 0.700, and 0.703, respectively. Ablation experiments verified the effectiveness of the CNN and GRU algorithms for the entire algorithm. Stator current and voltage were of the highest importance in the fault diagnosis model, followed by motor torque, and motor temperature was least important.
Contribution: The contribution of this paper lies in improving the recognition performance of fault types by combining two intelligent algorithms, CNN and GRU, and taking into account both local features and time-series features. It provides an effective reference for ensuring the stable operation of motor drive systems.

KEYWORDS

combined model, deep learning, faultdiagnosis, industrial automation control, permanent magnet synchronous motor

1 Introduction

In actual operation, a permanent magnet synchronous motor (PMSM) is prone to various faults due to factors such as electromagnetic interference, wear and tear, and load fluctuations. These faults will not only affect the operational efficiency and accuracy of the motor but also further cause safety accidents in the entire system (Pietrzak and Wolkiewicz, 2024; Huang et al., 2020; Ma et al., 2020). Therefore, it is necessary to monitor the operating status of the PMSM and diagnose faults in order

to maintain operational safety. Traditional PMSM diagnostic methods mainly rely on the analysis by physical models and human experience. These methods can identify some typical faults to a certain extent but have some drawbacks such as low diagnostic efficiency and accuracy, and difficulty in adapting to changes in complex operating conditions. In this context, deep learning techniques, leveraging their nonlinear modeling capabilities, offer new ideas for fault diagnosis of PMSM (Yi et al., 2025). Compared with traditional methods, deep learning technology has an advantage in dealing with high-dimensional, unstructured, time-series data; therefore, it is suitable for multi-source heterogeneous data collected in PMSM. Kang and Yao. (2024) proposed a fault diagnosis scheme for various fault conditions in PMSM systems and discovered that the proposed algorithm could accurately and reliably diagnose demagnetization faults and speed sensor faults under different severities of faults. Wang et al. (2024) applied a one-dimensional convolutional neural network (1D-CNN) to diagnose PMSM faults and found that this method could identify 11 types of motor faults, showing an accuracy of 99.7%. Ko et al. (2024) put forward a physically based approach for identifying demagnetization fault indicators in PMSMs without fractional harmonics in operation and found through simulation and experiments that the scheme was effective regardless of the operating conditions. Shen et al. (2025) proposed a static error elimination algorithm based on a proportional-integral controller and particle swarm optimization for electric vehicle drive systems. This algorithm was used for the robust predictive current control of PMSM. The experimental results showed that this algorithm has good dynamic adjustment performance and a small amount of calculation. Deng et al. (2024) carried out a study on a multi-objective energy management strategy for a parallel plug-in hybrid electric vehicle. They discovered that the improved control strategy can well balance the engine fuel economy and the battery temperature rise index, which has excellent battery state-of-charge maintenance ability. The above studies all conducted research on PMSM fault detection. Some of them used intelligent algorithms to identify fault types, while others analyzed the collected data and utilized their features to identify fault types. This paper also used an intelligent algorithm to identify PMSM faults. In this paper, in order to enhance the diagnostic performance of intelligent algorithms for PMSM faults, a convolutional neural network (CNN) and a gated recurrent unit (GRU) were combined. The CNN algorithm was used to extract the detailed features in the collected signals, and the GRU algorithm was used to obtain the rule features of the collected signals in the time series, so as to achieve a more accurate diagnosis of the types of faults. This paper collected normal and fault operation data from actual PMSMs for simulation experiments. The contribution of this paper lies in recognizing operation faults of PMSMs by combining a CNN with a GRU. The spatial features of fault data were extracted using the CNN, and the time-series features were extracted using the GRU. The two kinds of features were combined to achieve more accurate recognition of fault types.

2 Fault diagnosis of PMSM based on deep learning algorithms

Common PMSM fault types include stator winding faults, rotor faults, bearing faults, and control circuit anomalies (Li and Shi, 2024). All of these faults can lead to unstable motor output torque, reduced efficiency, increased noise, and, in severe cases, shutdown. Traditional PMSM fault diagnosis methods include physical model-based, signal processing-based, and rule-based threshold alarm methods. The first kind of methods build a PMSM simulation model to simulate different fault states and collect relevant parameters and uses the parameters obtained from the simulation to compare with the parameters of the actual motor (Zhang and Yu, 2022) for fault diagnosis.Signal processing-based methods extract the signal features of faults using various signal transformation algorithms to diagnose faults. Rule-based threshold alarm methods directly set the thresholds for the relevant parameters and determines the presence of a fault when the parameters exceed those threshold. The limitations of the diagnostic methods mentioned above are partly due to overly ideal setting conditions and high sensitivity to noise, and partly because fault judgment is too simplistic and crude (Yuan et al., 2022) to distinguish specific fault types.

In PMSM fault diagnosis, the advantage of deep learning technology lies in its ability to automatically extract features from collected data, its ability to handle high-dimensional, unstructured data, and the usability of the trained model in different operating conditions or motor models.

To enhance the performance of PMSM fault diagnosis, this paper chooses the CNN-GRU model (Wang et al., 2022). In this paper, sensors are used to collect relevant signals of a PMSM during operation. These signals can form a curve graph over time, thus the CNN algorithm can be used to extract features from it. The time-varying signals are also a kind of time series data; thus, GRU can be used for processing (Li et al., 2021a). The training process of the combined model for PMSM fault diagnosis (Figure 1) is as follows.

1. Sensors are used to collect data related to the determination of PMSM faults. In this paper, data such as stator current, stator voltage, temperature, and rotor torque of a PMSM are collected. The collected data are continuously segmented at certain time intervals, and the data collected in each period constitutes a sample, which is labeled according to the PMSM fault status at the time of collection.
2. The characteristic parameters that vary over time within each sample can form a curve graph, which is input into the CNN algorithm. The convolutional layer in the algorithm extracts the convolutional features from the curve graph. When extracting features, the convolution kernels in the convolutional layer move in the image at a set step size and perform the convolution operation (Zhang et al., 2021). The corresponding expression is shown in Equation 1:

$$y = f\left(\sum_{i,j} (x \cdot w)_{i,j} + b\right), \tag{1}$$

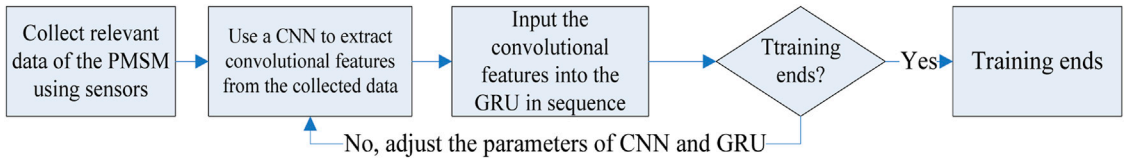

FIGURE 1
The training process of the CNN + GRU algorithm.

where y is the convolutional feature output by the convolutional layer, x is the input sample, w is a convolution kernel, b is a bias, $f(\ )$ is an activation function, and i and j are sample pixel coordinates. After extracting convolutional features, the pooling layer compresses the convolutional feature map to reduce the subsequent computational load. The pooling layer operates by moving the pooling box over the convolutional feature map at a fixed step size and compressing the data within the box. Max-pooling and mean-pooling are commonly used. The former uses the maximum value within the box as the compression result, while the latter uses the mean. The structure for the convolution and pooling of data images is set according to the requirements.

3. The extracted convolutional features are input into the GRU in chronological order for forward computation, and the forward computation formula in the GRU hidden layer is shown in Equation 2:

$$\begin{cases} z_t = f(\omega_z(h_{t-1}, x_t)) \\ r_t = f(\omega_r(h_{t-1}, x_t)) \\ h_t^{'} = \tanh(\omega(r_t \times h_{t-1}, x_t)) \\ h_t = (1 - z_t) \times h_{t-1} + z_t \times h_t^{'} \end{cases}, \quad (2)$$

where z_t is the output of the update gate, r_t is the output of the reset gate (Li et al., 2021b), ω_z and ω_r are the weight in the update and reset gates, x_t is the current input, i.e., the extracted convolutional feature of the current time, $f(\ )$ is the activation function used in the update and reset gates, h_{t-1} is the hidden state at the previous moment, $h_t^{'}$ is a temporary hidden state at the present moment, ω is the weight at the time of calculating $h_t^{'}$, and h_t is the hidden state at the current moment. The result obtained from the forward calculation in the hidden layer is input into the output layer to calculate the fault type probability distribution of samples using the softmax function. Finally, the fault type with the highest probability is output.

4. Whether the algorithm training is over is determined. If it is over, stop training the parameters of the fixed algorithm model; otherwise, reversely adjust the parameters of the algorithm model according to the loss function and return to step ②. The algorithm model used in this paper is designed to diagnose PMSM fault types and is a classification algorithm. Therefore, cross-entropy (Kim et al., 2020) is used as the loss function in this paper. The conditions for the algorithm training to stop include reaching a specified number of training sessions or having the loss function converge with fluctuations less than 10^{-8}.

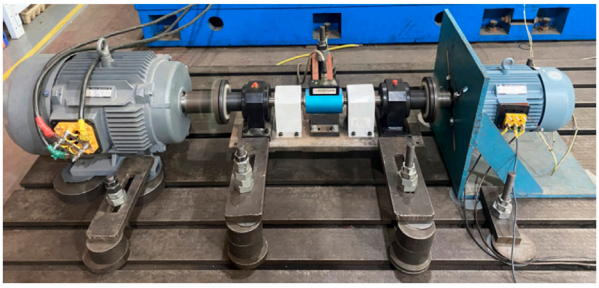

FIGURE 2
The PMSM device platform.

3 Simulation experiments

3.1 Experimental data

The experimental data were collected from an actual PMSM device. The PMSM device platform (Figure 2) contains two motors, namely, the test motor and the load motor, connected by a shaft coupling. The test motor is a PMSM, with the following parameters: 600 W rated power, 2.0 A rated current, two pole pairs, 0.63Wb flux link in the rotor permanent magnet, 0.16H straight-axis and cross-axis inductance, and 200 r/min rated speed.

For PMSM sample collection, current and voltage sensors were used to measure stator current and voltage during the operation of the test motor, temperature sensors were used to measure temperature, and torque sensors installed on shaft couplings were used to measure torque. The sampling frequency of each sensor was 40 kHz. When collecting samples from the PMSM in normal operation, the test motor speed was set to 50, 100, and 150 r/min, respectively, the load motor was not loaded or loaded with 2 Nm, and the sampling duration was 30 min. Before collecting samples from the PMSM with faulty stator windings, the additional winding taps of the test motor were artificially induced to simulate the inter-turn short-circuit fault in the stator windings. Before collecting samples from the PMSM with rotor faults, the rotor of the test motor was replaced with a rotor of uniform size but 10% eccentricity to simulate rotor eccentricity failure. Before collecting samples from the PMSM with bearing faults, the bearing of the test motor was replaced with one processed by electrical discharge machining. During the operation of the PMSM with the above-mentioned faults, the test motor speed was also set at 50, 100, and 150 r/min, no load and a load of 2 Nm were applied to the load motor respectively, and the sampling lasted for 30 min.

TABLE 1 Parameter settings for the fault diagnosis algorithm.

Structure	Parameter setting	Structure	Parameter setting
The input layer of the CNN	300 × 150	Convolutional layer 1 in the CNN	32 2 × 2-sized convolution kernels, with a moving step size of 1, sigmoid activation function
Pooling layer 1 in the CNN	A 2 × 2-sized pooling box, with a moving step size of 1, mean-pooling	Convolutional layer 2 in the CNN	64 2 × 2-sized convolution kernels, with a moving step size of 1, sigmoid activation function
Pooling layer 2 in the CNN	A 2 × 2-sized pooling box, with a moving step size of 1, mean-pooling	The hidden layer in the GRU	128 nodes, sigmoid activation function
The output layer in the GRU	Softmax function, four nodes	Number of training sessions	300 times
Learning rate	0.02	Learner	Adam

The data collected during normal operation and fault operation were split into lengths of one second, resulting in 1,800 samples for normal operation, 1,800 samples for stator winding inter-turn short circuit fault, 1,800 samples for rotor eccentricity fault, and 1,800 samples for bearing fault in the working condition of 50 r/min motor speed and no load. In working conditions such as "100 r/min motor speed and no load", "150 r/min motor speed and no load", "50 r/min motor speed and a load of 2 Nm", "100 r/min motor speed and a load of 2 Nm", and "150 r/min motor speed and a load of 2 Nm", the number of each type of sample was the same as that in the previous working condition. Finally, 43,200 samples were obtained. 60% of the samples were randomly selected from the sample set of each fault type in each working condition as training samples, and the remaining 40% were used as test samples.

3.2 Experimental methods

The relevant parameter settings of the CNN-GRU algorithm are shown in Table 1. In addition, to further verify the performance of this algorithm in fault diagnosis, comparisons were made with algorithms such as SVM, random forest (RF), and BPNN.

To verify the contributions of each part of the combined model algorithm adopted in this paper, an ablation experiment was conducted. The CNN and GRU parts were respectively eliminated for testing and comparison. A fully connected layer replaced the eliminated part. Finally, the Shapley additive explanations (SHAP) algorithm was used to measure the contribution of fault features to the algorithm model. The calculation formula of the SHAP algorithm is shown in Equation 3:

$$\begin{cases} f_X(S) = E\left[f(X) \mid X_S\right] \\ \Delta i(S) = f_X(S \cup \{i\}) - f_X(S) \\ \phi_i = \sum_S \dfrac{|S|!\,(N - |S| - 1)!}{N!} \cdot \Delta i(S), \\ g(x) = \phi_0 + \sum_{i=1}^{P} \phi_i \cdot z_i \end{cases} \tag{3}$$

where X denotes the data sample collected during PMSM operation, each sample has N features, four in this paper, S is a subset of sample feature set N without feature i, $f_X(S)$ denotes the expected value of the output of S, $\Delta i(S)$ is the marginal contribution of feature i after being added to S in the model's prediction results, ϕ_i is the SHAP value of feature i, $g(x)$ represents the constructed explanation function of feature contribution, ϕ_0 is the base value, i.e., the mean of the predicted model results, and z_i is an indicative parameter.

3.3 Evaluation indicator

The performance of the fault diagnosis algorithm was evaluated using the commonly used precision, recall rate, and F-score, as shown in Equation 4:

$$\begin{cases} P = \dfrac{TP}{TP + FN} \\ R = \dfrac{TP}{TP + FP}, \\ F = \dfrac{2 \cdot P \cdot R}{P + R} \end{cases} \tag{4}$$

where P is the precision, R is the recall rate, F is the combined value of precision and recall rate, TP indicates the actual number of cases, FP indicates the number of false positive cases, FN indicates the number of false negative cases, and TN represents the number of true negative cases.

3.4 Experimental results

The SVM, RF, BPNN, and the CNN-GRU algorithms were compared (Figure 3). It can be seen from the figure that the CNN-GRU algorithm exhibited the best fault-diagnosis performance for PMSM, followed by the BPNN algorithm, and the SVM and RF algorithms had the worst performance and differed little. It can be seen from Table 2 that the diagnostic performance of different diagnostic algorithms for the same type of faults was consistent with the overall trend. When the same diagnostic algorithm faced different types of faults, it can be seen that the diagnostic performance for inter-turn short-circuit faults in the stator winding was better. The reason for this is that the inter-turn short circuit of the winding directly affects the wire and directly reflects on the current and voltage values of the motor, which is relatively more intuitive. Rotor eccentricity and bearing faults cause motor vibration. During vibration, the distance between the

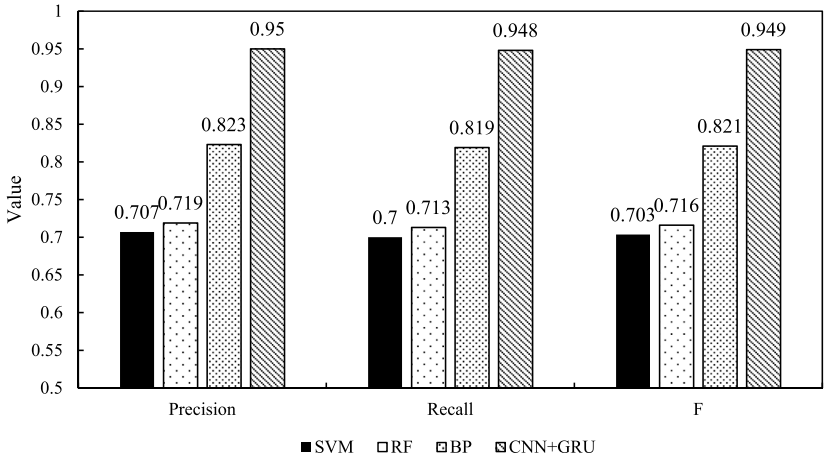

FIGURE 3
Performance comparison of algorithms.

TABLE 2 Diagnostic performance of four algorithms for different fault types.

Algorithm	Fault type	Precision	Recall rate	F-score
SVM	Stator winding inter-turn short circuit	0.721	0.719	0.720
	Rotor eccentricity	0.711	0.701	0.706
	Bearing fault	0.688	0.679	0.683
RF	Stator winding inter-turn short circuit	0.732	0.729	0.730
	Rotor eccentricity	0.721	0.712	0.716
	Bearing fault	0.703	0.699	0.701
BPNN	Stator winding inter-turn short circuit	0.848	0.843	0.845
	Rotor eccentricity	0.832	0.828	0.830
	Bearing fault	0.789	0.787	0.788
CNN-GRU	Stator winding inter-turn short circuit	0.976	0.973	0.974
	Rotor eccentricity	0.962	0.959	0.960
	Bearing fault	0.913	0.911	0.912

permanent magnet on the rotor and the stator winding coil will change unstably, affecting the current and voltage in the motor. But it is not as direct as the inter-turn short circuit.

To test the contributions of the CNN and GRU parts in the CNN-GRU model, ablation experiments were conducted. The CNN and GRU parts were respectively eliminated, and performance tests were conducted. It can be seen from Figure 4 that the diagnostic performance of the algorithm for PMSM faults was significantly reduced after removing the CNN or GRU parts, while the performance of fault diagnosis between the two algorithms with their respective parts removed was not much different.

The SHAP algorithm was employed to calculate the importance of the feature indicators in the model. Figure 5 shows that stator current and voltage were the most important in this model, followed by motor torque, and motor temperature was the least important. It can be seen that when the PMSM failed, the influence on stator current and voltage was most obvious, followed by motor torque, and finally motor temperature.

4 Discussion

PMSMs have gradually become the core executive components in key fields such as new-energy vehicle drive systems, industrial servo control, aerospace propulsion devices, and high-end numerical control equipment due to their excellent dynamic response performance. However, once a PMSM malfunctions and the fault is not diagnosed and addressed in a timely manner, it will not only lead to a decline in system performance and an increase in energy consumption but may also trigger a chain reaction of equipment damage and even safety accidents. Model-based analytical redundancy techniques and signal-processing-based feature-extraction methods are traditional PMSM fault-diagnosis

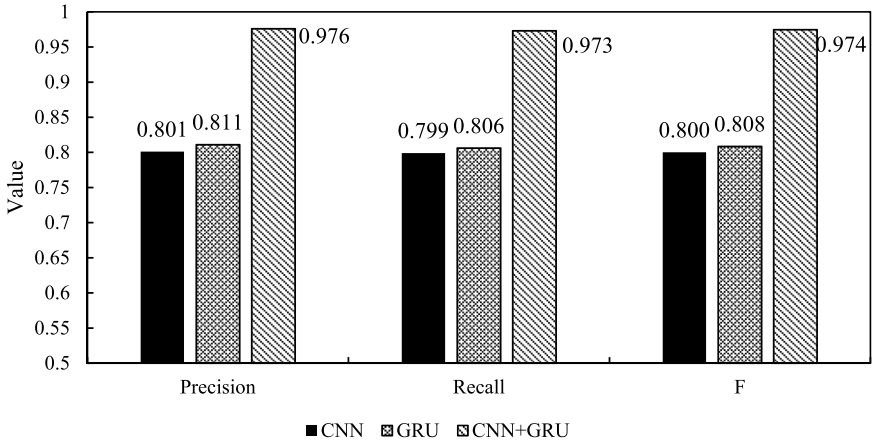

FIGURE 4
Results of the ablation experiments.

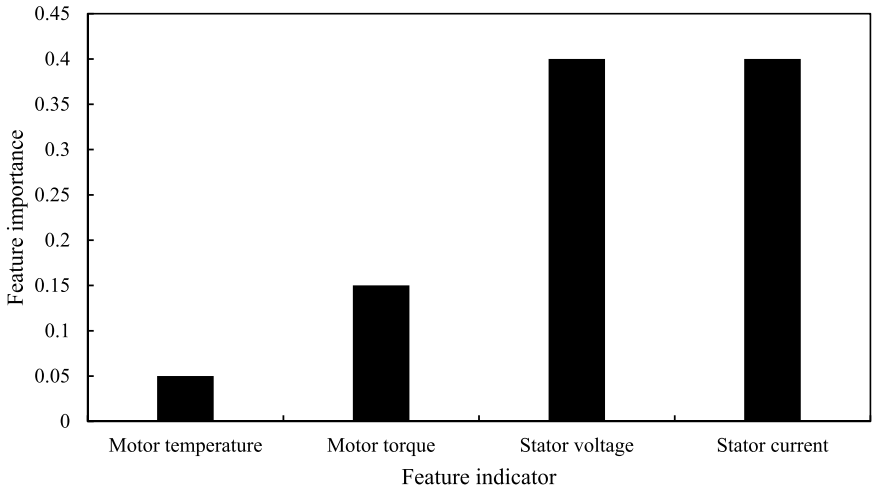

FIGURE 5
Importance of feature indicators in the fault diagnosis model.

methods. These methods are effective under specific operating conditions but have limitations. Firstly, they highly depend on accurate mathematical models. Secondly, the features designed manually are difficult to comprehensively reflect the non-linear characteristics of complex faults.

The CNN and GRU algorithms used in this paper are both deep learning algorithms with powerful nonlinear mapping capabilities. CNN can automatically extract the spatial features of data, and GRU can extract the features of data in the time series and implement an end-to-end learning paradigm. This paper combined a CNN with a GRU for the identification of PMSM fault types. In the simulation experiments, the CNN-GRU algorithm was compared with SVM, RF, and BPNN. Moreover, an ablation experiment was conducted. Finally, the SHAP algorithm was used to calculate the importance of feature indicators. The CNN-GRU algorithm exhibited better performance in identifying fault types compared with the other three algorithms. The results of the ablation experiment also verified that both the CNN part and the GRU part were effective for the algorithm. When a PMSM failed, the stator current and voltage were most significantly affected, followed by the motor torque, and finally the motor temperature. The reason is analyzed. The SVM algorithm is more suitable for processing data with linear regular features, and the RF algorithm is more suitable for processing data with discrete features. Although the BPNN algorithm is also a deep learning algorithm, it requires manual feature extraction during use. The CNN-GRU algorithm can automatically extract spatial and time-series features from data and use an activation function to fit the nonlinear rules.

5 Conclusion

This paper adopted a combination of CNN and GRU to diagnose PMSM faults. Then, normal and fault operation data

were collected from the actual PMSM for simulation experiments. The CNN-GRU algorithm was compared with the SVM, RF, and BPNN algorithms, and ablation experiments were conducted. Finally, the SHAP algorithm was used to calculate the importance of feature indicators in the algorithm model. The CNN-GRU algorithm showed superior fault-diagnosis performance than the other three algorithms. The results of the ablation experiment also confirmed that both the CNN and GRU parts were effective for the algorithm. When a fault occurred in the PMSM, the impact on the stator current and voltage was the most obvious, followed by the motor torque, and finally the motor temperature. The contribution of this paper lies in that the combination of CNN and GRU can fully utilize the spatial and temporal features of the data, thereby identifying the fault types more accurately and providing an effective reference for the fault diagnosis of PMSM.

The limitations of this paper included a limited number of algorithm models for comparison and insufficient analysis of feature importance using the SHAP algorithm. Therefore, future research will expand the range of algorithm models for comparison to verify the effectiveness of the proposed algorithm and to further analyze the relationship between feature indicators and different fault types.

Data availability statement

The original contributions presented in the study are included in the article/supplementary material, further inquiries can be directed to the corresponding author.

Author contributions

ZG: Software, Investigation, Supervision, Funding acquisition, Writing – review and editing, Conceptualization, Formal Analysis, Writing – original draft, Visualization, Data curation, Resources, Project administration, Methodology, Validation. XP: Writing – original draft, Resources, Investigation, Software, Writing – review and editing, Visualization, Methodology, Validation, Funding acquisition, Data curation, Conceptualization, Project administration, Supervision, Formal Analysis.

Funding

The author(s) declared that financial support was not received for this work and/or its publication.

Conflict of interest

The author(s) declared that this work was conducted in the absence of any commercial or financial relationships that could be construed as a potential conflict of interest.

Generative AI statement

The author(s) declared that generative AI was not used in the creation of this manuscript.

Any alternative text (alt text) provided alongside figures in this article has been generated by Frontiers with the support of artificial intelligence and reasonable efforts have been made to ensure accuracy, including review by the authors wherever possible. If you identify any issues, please contact us.

Publisher's note

References

Deng, T., Wu, S., Chen, Q., and Liu, P. (2024). Multi-objective energy management strategy for PHEVs based on working condition information prediction and time-varying equivalence factor ECMS. *Automot. Innov.* 7, 698–715. doi:10.1007/s42154-024-00298-9

Huang, W., Chen, H., and Zhao, Q. (2020). Fault diagnosis of inter-turn fault in permanent magnet-synchronous motors based on cycle-generative adversarial networks and deep autoencoder. *Appl. Sci.-Basel* 14 (5), 1–18. doi:10.3390/app14052139

Kang, Y., and Yao, L. (2024). Fault diagnosis for permanent magnet synchronous motor with demagnetization fault and sensor fault. *IEEE T. Instrum. Meas.* 73, 1–11. doi:10.1109/tim.2024.3460886

Kim, H., Park, Y., Oh, S. T., Jang, H., Bae, J. N., and Lee, J. (2020). Study on the offline inter-turn fault diagnosis according to the parameter of permanent magnet synchronous motor. *Trans. Korean Inst. Electr. Eng.* 69 (10), 1456–1463. doi:10.5370/kiee.2020.69.10.1456

Ko, Y., Lee, Y., Oh, J., Park, J., Chang, H., and Kim, N. (2024). Current signature identification and analysis for demagnetization fault diagnosis of permanent magnet synchronous motors. *Mech. Syst. Signal Pr.* 214, 1–18. doi:10.1016/j.ymssp.2024.111377

Li, H., and Shi, T. (2024). Diagnosis of inter-turn short-circuit incipient fault in permanent magnet synchronous motors using input current on the power side. *IEEE T. Ind. Inf.* 20 (12), 13741–13752. doi:10.1109/tii.2024.3431632

Li, F., Wang, Y., Xu, S., and Li, Y. (2021a). Fault diagnosis of permanent magnet synchronous motor inter turn short circuit based on deep reinforcement learning. *J. Phys. Conf. Ser.* 2137 (1), 012004. doi:10.1088/1742-6596/2137/1/012004

Li, T., Ma, R., and Zhang, Z. (2021b). Diagnosis of open-phase fault of five-phase permanent magnet synchronous motor by harmonic current analysis. *Microelectron. Reliab.* 126 (Nov.), 1–5. doi:10.1016/j.microrel.2021.114205

Ma, C., Gao, Y., Degano, M., Wang, Y., Fang, J., Gerada, C., et al. (2020). Eccentric position diagnosis of static eccentricity fault of external rotor permanent magnet synchronous motor as an in-wheel motor. *IET Electr. Power App.* 14 (11), 2263–2272. doi:10.1049/iet-epa.2019.0617

Pietrzak, P., and Wolkiewicz, M. (2024). Condition monitoring and fault diagnosis of permanent magnet synchronous motor stator winding using the continuous wavelet transform and machine learning. *Power Elect. Drives* 9 (1), 106–121. doi:10.2478/pead-2024-0007

Shen, L., Zhang, J., Chen, K., and Wen, X. (2025). A static current error elimination algorithm for predictive current control in PMSM for electric vehicles. *Green Energy Intell. Transp.* 5, 100306. doi:10.1016/j.geits.2025.100306

Wang, J., Wei, L., and Wang, M. (2022). A fault diagnosis method of turn-to-turn short circuit of permanent Magnet Synchronous motor (PMSM) based on deep learning. *Proc. SPIE* 12506, 1–11. doi:10.1117/12.2662616

Wang, M. H., Chan, F. C., and Lu, S. D. (2024). Fault diagnosis of permanent magnet synchronous motor based on 1D-Convolutional neural network. *Sensors Mater* 36 (5), 2597–2612. doi:10.18494/sam4834

Yi, C. P., Lin, Y. J., Ho, P. J., and Yang, S. C. (2025). Magnet fault diagnosis for permanent magnet synchronous motor based on flux estimation with PWM voltage measurement. *IEEE T. Ind. Electron.* 72 (2), 2100–2110. doi:10.1109/tie.2024.3426031

Yuan, M., Yin, Z., Zhang, Y., and Zhang, Z. (2022). "Diagnosis method of IGBT open circuit fault of permanent magnet synchronous motor driver based on MPCC," in *2022 IEEE international power electronics and application conference and exposition (PEAC)*, 622–626.

Zhang, M., and Yu, Y. Q. (2022). Demagnetization fault diagnosis of permanent magnet synchronous motor based on empirical mode decomposition. *J. Phys. Conf. Ser.* 2395 (1), 012031. doi:10.1088/1742-6596/2395/1/012031

Zhang, Y., Liu, G., Zhao, W., Zhou, H., Chen, Q., and Wei, M. (2021). Online diagnosis of slight interturn short-circuit fault for a low-speed permanent magnet synchronous motor. *IEEE T. Transp. Electr.* 7 (1), 104–113. doi:10.1109/tte.2020.2991271